Available online at www.sciencedirect.com
ScienceDirect
C. R. Physique 10 (2009) 447–463
COMPTES RENDUS PHYSIQUE

Metamaterials / Métamatériaux

Time-reversed waves and super-resolution

Mathias Fink *, Julien de Rosny, Geoffroy Lerosey, Arnaud Tourin

Institut Langevin, École supérieure de physique et de chimie industrielle de la ville de Paris, UMR CNRS 7587, 10, rue Vauquelin, 75005 Paris, France

Available online 22 August 2009

Abstract

Time-reversal mirrors (TRMs) refocus an incident wavefield to the position of the original source regardless of the complexity of the propagation medium. TRMs have now been implemented in a variety of physical scenarios from GHz microwaves to MHz ultrasonics and to hundreds of Hz in ocean acoustics. Common to this broad range of scales is a remarkable robustness exemplified by observations at all scales that the more complex the medium (random or chaotic), the sharper the focus. A TRM acts as an antenna that uses complex environments to appear wider than it is, resulting for a broadband pulse, in a refocusing quality that does not depend on the TRM aperture.

Moreover, when the complex environment is located in the near field of the source, time-reversal focusing opens completely new approaches to super-resolution. We will show that, for a broadband source located inside a random metamaterial, a TRM located in the far field radiated a time-reversed wave that interacts with the random medium to regenerate not only the propagating but also the evanescent waves required to refocus below the diffraction limit. This focusing process is very different from that developed with superlenses made of negative index material only valid for narrowband signals. We will emphasize the role of the frequency diversity in time-reversal focusing. ***To cite this article: M. Fink et al., C. R. Physique 10 (2009).***

Résumé

Champs retournés temporellement et super-résolution. Les miroirs à retournement temporel (MRT) refocalisent une onde incidente sur la position de la source initiale indépendamment de la complexité du milieu de propagation. Les MRTs ont maintenant été mis en œuvre dans des situations physiques variées depuis les microondes GHz jusqu'aux ondes ultrasonores MHz en passant par l'acoustique sous-marine à quelques centaines de Hz. Leur robustesse commune à toutes ces fréquences est illustrée par le fait que pour toutes ces échelles plus le milieu est complexe (aléatoire ou chaotique) plus la focalisation est fine. Un MRT agit comme une antenne qui utilise l'environnement complexe pour paraître plus large qu'elle ne l'est, de telle manière que, pour une impulsion large bande, la finesse de la refocalisation ne dépende pas de l'ouverture du MRT.

De plus, lorsque l'environnement complexe se situe dans le champ proche de la source, la focalisation par retournement temporel ouvre une toute nouvelle approche de la super-résolution. Nous verrons que pour une source large bande située dans un métamatériau aléatoire, un MRT situé en champ lointain rayonne un champ retourné temporellement qui interagit avec le milieu aléatoire pour recréer non seulement les ondes propagatives mais aussi les ondes évanescentes nécessaires à la focalisation au-delà de la limite de diffraction. Ce processus de focalisation est très différent de celui développé avec les super-lentilles faites de matériau d'indice négatif, valable seulement pour des signaux à bande étroite. Nous soulignerons le rôle de la diversité fréquentielle dans le retournement temporel. ***Pour citer cet article : M. Fink et al., C. R. Physique 10 (2009).***

* Corresponding author.
E-mail address: mathias.fink@espci.fr (M. Fink).

1631-0705/$ – see front matter
doi:10.1016/j.crhy.2009.07.003

Keywords: Time-reversal mirror; Metamaterials

Mots-clés : Miroir à retournement temporel ; Métamatériaux

1. Introduction

Time-reversal invariance of the wave equation in acoustics and electromagnetisms allows one to build time-reversal mirrors (TRMs) made of arrays of reversible antenna, allowing an incident broadband wavefield to be sampled, recorded, time-reversed and re-emitted. TRMs refocus the incident wavefield to the position of the original source regardless of the complexity of the propagation medium. The first TRMs have been developed in the field of acoustics [1–3]. An acoustic source, located inside a lossless medium, radiates a brief transient pulse that propagates and is potentially distorted by the medium. Time reversal of the acoustic field would entail the reversal, at some instant, of every particle velocity in the medium. This kind of instantaneous time reversal in the whole volume is practically impossible to achieve. A more realistic alternative can be developed thanks to the Helmholtz–Kirchoff integral theorem. The acoustic field radiated by a source could be measured on every point of an enclosing surface (acoustic retina), and retransmitted in time-reversed order, then the wave will travel back to its source, see Fig. 1. Both time-reversal invariance and spatial reciprocity [4] are required to reconstruct a time-reversed wave in the entire volume by means of this two-dimensional time-reversal operation. From an experimental point of view a closed TRM consists of a two-dimensional piezoelectric transducer array that samples the wavefield over a closed surface. An array pitch of the order of $\lambda/2$ where λ is the smallest wavelength of the pressure field is needed to ensure the recording of all the information on the wavefield. Each transducer is connected to its own electronic circuitry that consists of a receiving amplifier, an A/D converter, a storage memory and a programmable transmitter able to synthesize a time-reversed version of the stored signal.

In practice, closed TRMs are difficult to realize and the TR operation is usually performed on a limited angular area, thus apparently limiting focusing quality. A TRM consists typically of a small number of elements or time-reversal channels. The major interest of TRM, compared to classical focusing devices (lenses and beam forming) is certainly the relation between the medium complexity and the size of the focal spot. A TRM acts as an antenna that uses complex environments to appear wider than it is, resulting in a refocusing quality that does not depend on the TRM aperture.

One spectacular result that is shown in this article deals with a complex environment located in the near field of the source. Such an environment can be made, for example, of a random or periodic distribution of resonating scatterers with a mean distance smaller than the wavelength. It will be shown that, for a broadband source located inside such random metamaterials, a TRM located in the far field radiated a time-reversed wave that interacts with the random medium to regenerate not only the propagating but also the evanescent waves required to refocus below the diffraction limit. This focusing process is very different from that developed with superlenses made of negative index material only valid for narrowband signals. We will emphasize the role of the frequency diversity in time-reversal focusing.

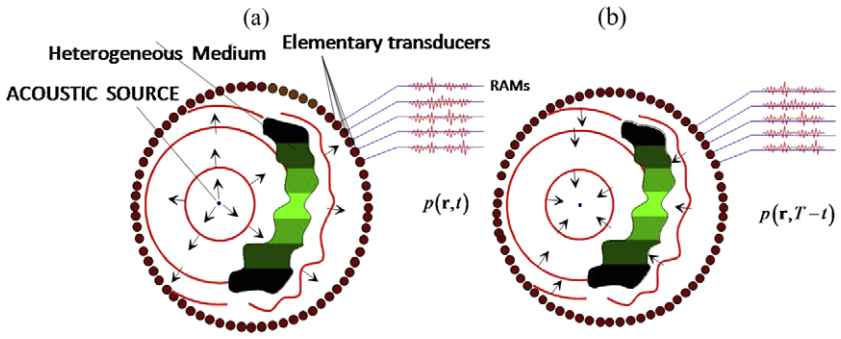

Fig. 1. (a) Recording step: A closed surface is filled with transducer elements. A point-like source generates a wavefront which is distorted by heterogeneities. The distorted pressure field is recorded on the cavity elements. (b) Time-reversed or reconstruction step: The recorded signals are time-reversed and reemitted by the cavity elements. The time-reversed pressure field back-propagates and refocuses exactly on the initial source.

2. Time reversal of acoustics waves: basic principles

The basic theory employs a scalar wave formulation $p(\mathbf{r},t)$ and, hence, is strictly applicable to acoustic or ultrasound propagations in fluids. However, the basic ingredients and conclusions apply equally well to elastic waves in solids and to electromagnetic fields.

Let us consider the propagation of an acoustic wave in a heterogeneous and non-dissipative medium, whose compressibility $\kappa(\mathbf{r})$ and density $\rho(\mathbf{r})$ vary in space. By introducing the sound speed $c(\mathbf{r}) = (\rho(\mathbf{r})\kappa(\mathbf{r}))^{-1/2}$, one can obtain the wave propagation equation for a given pressure field $p(\mathbf{r},t)$:

$$\vec{\nabla}\cdot\left(\frac{\vec{\nabla}p(\mathbf{r},t)}{\rho(\mathbf{r})}\right) - \frac{1}{\rho(\mathbf{r})c(\mathbf{r})^2}\frac{\partial^2 p(\mathbf{r},t)}{\partial t^2} = 0 \tag{1}$$

One can notice the particular behaviour of this wave equation regarding the time variable t. Indeed, it only contains a second-order time derivative operator. This property is the starting point of the time-reversal principle. A straightforward consequence of this property is that if $p(\mathbf{r},t)$ is a solution of the wave equation, then $p(\mathbf{r},-t)$ is also solution of the problem. This property illustrates the invariance of the wave equation during a time-reversal operation, the so-called time-reversal invariance. However, this property is only valid in a non-dissipative medium. If wave propagation is affected by dissipation effects, odd order time derivatives appear in the wave equation and the time-reversal invariance is lost. Nevertheless, one should note here that if the ultrasonic absorption coefficient is sufficiently small in the frequency bandwidth of the ultrasonic waves used for the experiments, the time-reversal invariance remains valid.

In any propagation experiment, the acoustic sources and the boundary conditions determine a unique solution $p(\mathbf{r},t)$ in the fluid. The goal, in time-reversal experiments, is to modify the initial conditions in order to generate the dual solution $p(\mathbf{r},T-t)$ where T is a delay due to causality requirements. Cassereau and Fink [4] and Jackson and Dowling [5] have studied theoretically the conditions necessary to insure the generation of $p(\mathbf{r},T-t)$ in the entire volume of interest.

2.1. An ideal time-reversal experiment

Although reversible acoustic retinas usually consist of discrete elements, it is convenient to examine the behaviour of idealized continuous retinas, defined by two-dimensional surfaces. In the case of a time-reversal cavity, we assume that the retina completely surrounds the source.

In a first step, let us consider a point-like source located at $\mathbf{r}_0$ inside a volume V surrounded by a surface S, emitting a time modulation $s(t)$. The inhomogeneous wave equation is given by

$$\vec{\nabla}\cdot\left(\frac{\vec{\nabla}p(\mathbf{r},t)}{\rho}\right) - \frac{1}{\rho c^2}\frac{\partial^2 p(\mathbf{r},t)}{\partial t^2} = -\delta(\mathbf{r}-\mathbf{r}_0)s(t) \tag{2}$$

Note that contrary to Eq. (1), the right part of this equation describes the source term and this term may contain spatial and time singularities. Considering, for example, an impulsive source $s(t) = \delta(t)$ at time 0, the causal solution to Eq. (2) reduces to the retarded Green's function $G_{ret}(\mathbf{r},\mathbf{r}_0;t)$ that takes into account the heterogeneities and the boundaries of the medium. Note that to respect causality, only the causal Green's function (retarded) that satisfies the Sommerfeld radiation boundary condition at infinity is selected while the advanced Green's function (the anti causal) is neglected.

The initial goal of a perfect time-reversed experiment is to generate in the medium this advanced Green's function $G_{adv}(\mathbf{r},\mathbf{r}_0;t) = G_{ret}(\mathbf{r},\mathbf{r}_0;-t)$ by modifying the initial conditions on the boundaries of the experiment. This would be an optimal way to obtain super-resolution in a focusing experiment, because the advanced Green's function converges towards a spatial singularity. In a more realistic way, taking into account any source modulation $s(t)$ with a well defined bandwidth, we are interested to generate in the volume of the experiment $p(\mathbf{r},-t)$.

The so-called time-reversal cavity approach was developed, by using the fact that a wavefield at any location inside a volume V (without source) can be predicted from the knowledge of both *the field and its normal derivative* on the surrounding surface S. Therefore a time-reversal experiment can be conceived in the following way: During the second step of the time-reversal process, the initial source at $\mathbf{r}_0$ is removed and we create on the surface of the cavity

monopole and dipole sources that correspond to the time reversal of those same components measured during the first step. The time-reversal operation is described by the transform $t \to -t$ and the secondary sources are

$$\begin{cases} p_s(\mathbf{r}, t) = G(\mathbf{r}, \mathbf{r}_0; -t) \otimes s(-t) \\ \partial_n p_s(\mathbf{r}, t) = \partial_n G(\mathbf{r}, \mathbf{r}_0; -t) \otimes s(-t) \end{cases} \tag{3}$$

where we use now and in the following the notation $G(\mathbf{r}, \mathbf{r}_0; t)$ instead of $G_{ret}(\mathbf{r}, \mathbf{r}_0; t)$ and neglect the causal delay T needed to record and reemit the signals.

Due to these secondary sources on S, the time-reversed pressure field $p_{tr}(\mathbf{r}, t)$ propagates backwards inside the cavity. It can be calculated using a modified version of the Helmholtz–Kirchhoff integral, valid inside a zone without source:

$$p_{tr}(\mathbf{r}, t) = \int_{-\infty}^{+\infty} \mathrm{d}t' \iint_S \left[G(\mathbf{r}, \mathbf{r}'; t - t') \partial_n p_s(\mathbf{r}', t') - p_s(\mathbf{r}', t') \partial_n G(\mathbf{r}, \mathbf{r}'; t - t') \right] \frac{\mathrm{d}^2 \mathbf{r}'}{\rho(\mathbf{r}')} \tag{4}$$

Instead of directly computing this integral, there is a straightforward way to predict the field $p_{tr}(\mathbf{r}, t)$. Our initial goal was to radiate inside the volume surrounded by surface S the field $p(\mathbf{r}, -t) = G(\mathbf{r}, \mathbf{r}_0; -t) \otimes s(-t)$ with $G(\mathbf{r}, \mathbf{r}_0; -t)$ the advanced Green's function. However, the wave equation verified by $p(\mathbf{r}, -t)$ in the volume V can be obtained by changing t in $-t$ in Eq. (2)

$$\vec{\nabla} \cdot \left(\frac{\vec{\nabla} p(\mathbf{r}, -t)}{\rho} \right) - \frac{1}{\rho c^2} \frac{\partial^2 p(\mathbf{r}, -t)}{\partial t^2} = -\delta(\mathbf{r} - \mathbf{r}_0) s(-t) \tag{5}$$

Therefore, to obtain a perfect time-reversal field would require also that the original active source that injected energy into the system in the initial step be replaced by a *sink* (the time reversal of a source) that corresponds to the right term of Eq. (4). This means that to achieve a perfect time reversal, both *the source has to be transformed into a sink*, while the *field and its normal derivative on surface S has also to be time-reversed* (like in Eq. (4)). The superposition of these two fields will give exactly $p(\mathbf{r}, -t)$. Therefore $p(\mathbf{r}, -t)$ is given by the following sum

$$p(\mathbf{r}, -t) = p_{tr}(\mathbf{r}, t) + G(\mathbf{r}, \mathbf{r}_0; t) \otimes s(-t) \tag{6}$$

For a source term with a Dirac excitation, we directly get for the time-reversed field:

$$p_{tr}(\mathbf{r}, t) = G(\mathbf{r}, \mathbf{r}_0; -t) - G(\mathbf{r}, \mathbf{r}_0; t) \tag{7}$$

This important result is, in some way, disappointing because it means that reversing an acoustic field using a closed TRM is not enough to radiate only the advanced wavefield. Complete time reversal requires not only to time-reverse the source but the original source as well. Eq. (7) can be interpreted as the difference of advanced and retarded waves centered on the initial source position. The converging wave (advanced) collapses at the origin and is followed by a diverging (retarded) wave. Thus the time-reversed field observed as a function of time shows two wavefronts of opposite sign. The wave re-emitted by the time-reversal cavity looks like a convergent wavefield during a given period, but a wavefield which *does not know how to stop.* When the converging wavefield reaches the location of the initial source location, it collapse and then continues its propagation as a diverging wavefield.

To achieve a perfect time reversal both the field on the surface of the cavity has to be time-reversed, and the source has to be transformed into a sink [6,7]. In this manner one may achieve time-reversed focusing below the diffraction limit. The role of the new source term $-\delta(\mathbf{r} - \mathbf{r}_0) s(-t)$ in Eq. (5) is to transmit a diverging wave that exactly cancels the outgoing spherical wave.

In a monochromatic approach, taking into account the evanescent wave concept, the necessity of replacing a source by a sink in the complete time-reversed operation can be interpreted as follows. In the first step a point-like source of size much smaller than a wavelength radiates a field that can be described as a superposition of homogeneous plane waves propagating in the various directions $\vec{k}$ and of decaying, non-propagating, evanescent plane waves [8]. The evanescent waves contain information on fine scale features of the source; they decay exponentially with distance and do not contribute in the far field. If the TRM is located in the far field of the source, the time-reversed field retransmitted by the mirror does not contain these evanescent components. The role of the sink is to radiate exactly, with the good timing, the evanescent waves that have been lost during the first step. The resulting field contains the evanescent part that is needed to focus below diffraction limits. Time reversal below the diffraction limit has been

experimentally demonstrated in acoustics, using an acoustic sink placed at the focal point. Focal spots of size $\lambda/14$ have been observed by de Rosny and Fink [6]. One drawback is the need to use an active source at the focusing point to exactly cancel the usual diverging wave created during the focusing process.

2.2. Time reversal in free space

For example, in the case of a *homogeneous* medium, assuming that the retina does not perturb the field propagation (free-space assumption), the free-space retarded Green's function G_0 reduces to a diverging spherical impulse wave that depends only on $\mathbf{r}-\mathbf{r}_0$ and propagates with a sound speed c. Thus, neglecting the causal time delay T, the time-reversed field can be written as:

$$p_{tr}(\mathbf{r},t) \prec \left\{ \frac{1}{4\pi|\mathbf{r}-\mathbf{r}_0|}\delta\left(t+\frac{|\mathbf{r}-\mathbf{r}_0|}{c}\right) - \frac{1}{4\pi|\mathbf{r}-\mathbf{r}_0|}\delta\left(t-\frac{|\mathbf{r}-\mathbf{r}_0|}{c}\right)\right\} \otimes s(-t) \tag{8}$$

that reduces to the time derivative of the source modulation at the origin:

$$p_{tr}(\mathbf{r}=\mathbf{r}_0,t) = -\frac{1}{2\pi c}s'(-t) \tag{9}$$

In the case of a narrowband excitation (monochromatic excitation of pulsation ω), the interference between the converging and the diverging fields leads to the classical diffraction limits. Indeed, by calculating the Fourier transform of Eq. (7) over the time variable t, we obtain

$$\hat{P}_{tr}(\mathbf{r},\omega) = \frac{\exp(-jk|\mathbf{r}-\mathbf{r}_0|)}{4\pi|\mathbf{r}-\mathbf{r}_0|} - \frac{\exp(jk|\mathbf{r}-\mathbf{r}_0|)}{4\pi|\mathbf{r}-\mathbf{r}_0|} = -2j\frac{\sin(k|\mathbf{r}-\mathbf{r}_0|)}{4\pi|\mathbf{r}-\mathbf{r}_0|} = -2j\,\mathrm{Im}\,\hat{G}(\mathbf{r}-\mathbf{r}_0,\omega) \tag{10}$$

where $j^2=-1$. The time-reversed field at initial source position is finite because it is the difference between a converging and a diverging wave and not the sum (otherwise it will have a discontinuity there).

As a consequence, the time-reversed field is focused on the initial source position, with a focal spot size limited to one half-wavelength π/k that corresponds to the standard formulation for the complex field modulus, where k is the wavenumber and $\hat{G}(\mathbf{r}-\mathbf{r}_0,\omega)$ is the monochromatic Green's function. The point spread function is proportional to the imaginary part of the monochromatic Green's function.

2.3. Time reversal through heterogeneous medium

In the case of a non-dissipative heterogeneous medium surrounding the source, a similar interpretation can be given, but the retarded Green's function $\hat{G}(\mathbf{r},\mathbf{r}_0;\omega)$ is no longer dependent on $\mathbf{r}-\mathbf{r}_0$, but is now a function separately of both $\mathbf{r}$ and $\mathbf{r}_0$, taking into account, for example multiple scattering processes between heterogeneities

$$\hat{P}_{tr}(\mathbf{r},\omega) = \iint_S \left[\partial_n\hat{G}^*(\mathbf{r}',\mathbf{r}_0;\omega)\hat{G}(\mathbf{r},\mathbf{r}';\omega) - \hat{G}^*(\mathbf{r}',\mathbf{r}_0;\omega)\partial_n\hat{G}(\mathbf{r},\mathbf{r}';\omega)\right]\frac{\mathrm{d}^2\mathbf{r}'}{\rho(\mathbf{r}')} = -2j\,\mathrm{Im}\,\hat{G}(\mathbf{r},\mathbf{r}_0;\omega) \tag{11}$$

Note that the field amplitude at the focal point is directly proportional to the LDOS, the so-called *local density of states* that depends on the medium complexity around the source point. In the situation where the source is located inside a periodic or random metamaterial with scatterers closed to the source, it can happen that the LDOS be zero for some source position and therefore the time-reversed wave will have a node at the source point. However, for broadband excitation, the resulting field take advantage of the frequency diversity.

For a broadband excitation $s(t)$ the time-reversed field is given by:

$$p_{tr}(\mathbf{r},t) = -2j\int \mathrm{Im}\,\hat{G}(\mathbf{r},\mathbf{r}_0;\omega)S^*(\omega)\exp(j\omega t)\,\mathrm{d}\omega \tag{12}$$

where $S(\omega)$ is the Fourier transform of the source modulation. For an excitation with a flat bandwidth $\Delta\omega$, the field at the collapse time ($t=0$) reads

$$p_{tr}(\mathbf{r},t=0) = -2j\int_{\Delta\omega} \mathrm{Im}\,\hat{G}(\mathbf{r},\mathbf{r}_0;\omega)\,\mathrm{d}\omega \tag{13}$$

Therefore the time-reversed field at the focus (source point) and at the collapse time is given by

$$p_{tr}(\mathbf{r}=\mathbf{r}_0, t=0) = -2j \int_{\Delta\omega} \operatorname{Im} \hat{G}(\mathbf{r}_0, \mathbf{r}_0; \omega)\, \mathrm{d}\omega \tag{14}$$

Thus, the time-reversed field at the source point and at the focal time is directly proportional to the number of modes excited by the source.

2.4. An experimental point of view

From an experimental point of view, it is difficult to measure both the field and its normal derivative at any point of surface S. Experiments are carried out with transducer arrays that behave either as monopolar or as dipolar transducers and that spatially sample the receiving and emitting surface. Assuming that the time-reversal retina consists of discrete elements located at position $\mathbf{r}_i$ in the *far field* of the source, the observation points and the heterogeneities, a paraxial approximation, allows one to replace the field normal derivative by time derivative and the integration over S in Eq. (4) is replaced by summation over N surface element positions:

$$p_{tr}(\mathbf{r}, t) = C \frac{\partial}{\partial t} \sum_{i=1}^{N} G(\mathbf{r}_i, \mathbf{r}_0; -t) \otimes G(\mathbf{r}, \mathbf{r}_i; t) \tag{15}$$

where C is a scaling factor.

3. TRM in complex media

It is generally difficult to use acoustic arrays that completely surround the area of interest, so the closed cavity is usually replaced by a TRM of finite angular aperture. This yields an increase of the point spread function that is related to the limited angular size of the mirror observed from the source. In the standard theory of diffraction in homogeneous free space, the point-spread function is related to the angular spectrum of the aperture. For a closed time-reversal mirror, the $\vec{k}$ vectors of the radiated field span the whole 4π solid angle and the focal spot dimension is minimal ($\lambda/2$). When a TRM covers a limited solid angle, the spatial diversity of $\vec{k}$ vectors that interact with the TRM is reduced. Therefore the focal spot size is increased.

The main interest of focusing with TRM is that in media with complex structure the spatial diversity of the $\vec{k}$ vectors captured by a small TRM can be significantly increased. Wave propagation in media with complex boundaries or random scattering medium can increase the apparent aperture of the TRM, resulting in a focal spot size smaller than that predicted by classical formulas.

The basic idea is to replace one part of the transducers needed to sample a closed time-reversal surface by reflecting boundaries that redirect one part of the incident wave towards the TRM aperture (see Fig. 2). When a source radiates a wavefield inside a closed cavity or in a waveguide, multiple reflections along the medium boundaries can significantly increase the apparent aperture of the TRM. Thus spatial information on the $\vec{k}$ vectors that is usually lost with a finite aperture TRM is converted into the time domain. The reversal quality then depends crucially on the duration of the time-reversal window, i.e., the length of the recording that is reversed.

Such a concept is strongly related to a kaleidoscopic effect that appears thanks to the multiple reverberations on the waveguide boundaries. Waves emitted by each transducer are multiply reflected, creating at each reflection 'virtual' transducers that can be observed from the desired focal point. Thus we create a large virtual array from a limited number of transducers and a small number of transducers is multiplied to create a "kaleidoscopic" transducer array. Two different examples will be presented (a chaotic cavity and a multiply scattering medium).

3.1. One-channel time reversal in chaotic cavities

In this paragraph, we are interested in multiply reflected waves: waves confined in closed reflecting cavities with non-symmetrical geometry. With closed boundary conditions, no information can escape from the system and a reverberant acoustic field is created. If, moreover, the geometry of the cavity shows ergodic and mixing properties, one may hope to collect all information at only one point. Ergodicity means that, due to the boundary geometry, any

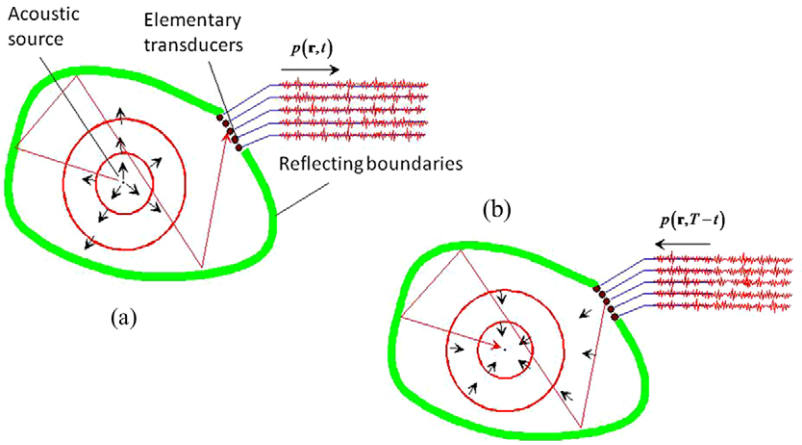

Fig. 2. One part of the transducers is replaced by reflecting boundaries. In (a) the wave radiated by the source is recorded by a set of transducers through the reverberation inside the cavity. In (b), the recorded signals are time-reversed and reemitted by the transducers.

acoustic ray radiated by a point source and multiply reflected would pass every location in the cavity. Therefore, all the information about the source can be redirected towards a single time-reversal transducer. This is the regime of fully diffuse wavefields that can be also defined as in room acoustics as an uncorrelated and isotropic mix of plane waves of all propagation directions [9,10]. Draeger and Fink [11–13] showed experimentally and theoretically that in this particular case a time-reversal focusing with $\lambda/2$ spot can be obtained *using only one TR channel* operating in a closed cavity.

The first experiments were made with elastic waves propagating in a 2-D cavity with negligible absorption. They were carried out using guided elastic waves in a monocrystalline D-shaped silicon wafer known to have chaotic ray trajectories. This property eliminates the effective regular gratings of the previous section. Silicon was selected also for its weak absorption. Elastic waves in such a plate are akin to Lamb waves.

An aluminum cone coupled to a longitudinal transducer generated waves at one point of the cavity. A second transducer was used as a receiver. The central frequency of the transducers was 1 MHz and their relative bandwidth was 100% ($\Delta\omega = 1$ MHz). At this frequency, only three propagating modes are possible (one flexural, one quasi-extensional, one quasi-shear). The source was considered point-like and isotropic because the cone tip is much smaller than the central wavelength. A heterodyne laser interferometer measures the displacement field as a function of time at different points on the cavity. Assuming that there is no mode conversion at the boundaries between the flexural mode and other modes, we have only to deal with one field, the flexural-scalar field.

The experiment is a "two-step process" as described above: In the first step, one of the transducers, located at point $\mathbf{r}_0$ (Fig. 3), transmits a short omnidirectional signal of duration 0.5 μs. Another transducer, located at $\mathbf{r}_{trm}$, observes a long random-looking signal that results from multiple reflections of along the boundaries of the cavity. It continues for more than 50 ms corresponding to some hundred reflections at the boundaries. Then, a portion ΔT of the signal is selected, time-reversed and re-emitted by point $\mathbf{r}_{trm}$. As the time-reversed wave is a flexural wave that induces vertical displacements of the silicon surface, it can be observed using the optical interferometer that scan the surface on different observation points $\mathbf{r}$ around point $\mathbf{r}_0$ (see Fig. 3).

For time-reversal windows of sufficiently long duration ΔT, one observes both an impressive time recompression at point $\mathbf{r}_0$ and a refocusing of the time-reversed wave around the origin (see Figs. 4a and 4b for $\Delta T = 1$ ms), with a focal spot whose radial dimension is equal to half the wavelength of the flexural wave. Using reflections at the boundaries, the time-reversed wavefield converges towards the origin from all directions and gives a circular spot, like the one that could be obtained with a closed time-reversal cavity covered with transducers. A complete study of the dependence of the spatio-temporal side lobes around the origin shows a major result (Draeger et al. [13]): a time duration ΔT of nearly 1 ms is enough to obtain a good focusing. For values of ΔT larger than 1 ms, the sidelobes' shape and the signal-to-noise ratio (focal peak/sidelobes) do not improve further. There is a saturation regime. Once the saturation regime is reached, point $\mathbf{r}_{trm}$ will receive redundant information. The saturation regime is reached after a time $\tau_{Heisenberg}$ called the Heisenberg time. It is the minimum time needed to resolve the eigenmodes in the cavity. It can also be interpreted as the time it takes for all a single ray to reach the vicinity of any point in the cavity within

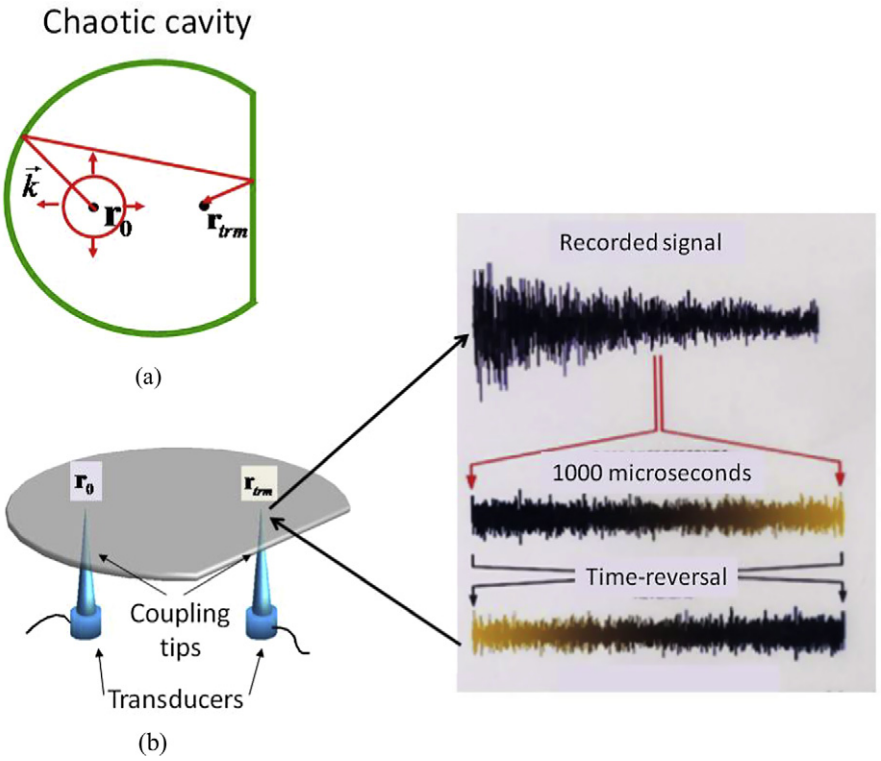

Fig. 3. (a) Geometry of the chaotic cavity. (b) Time-reversal experiment conducted in a chaotic cavity with flexural waves. In a first step, a point transducer located at point $\mathbf{r}_0$ transmits a 1 μs long signal. The signal is recorded at point $\mathbf{r}_{trm}$ by a second transducer. The signal spreads on more than 30 ms due to reverberation. In the second step of the experiment, a 1 ms portion of the recorded signal is time-reversed and retransmitted back in the cavity.

a distance $\lambda/2$. This guarantees enough interference between all the multiply reflected waves to build each of the eigenmodes in the cavity. The mean distance $\delta\omega$ between the eigenfrequencies is related to the Heisenberg time; $\tau_{Heisenberg} = \frac{1}{\delta\omega}$.

The success of this time-reversal experiment in a closed chaotic cavity is particularly interesting with respect to two aspects. Firstly, it proves the feasibility of acoustic time reversal in cavities of complex geometry that give rise to chaotic ray dynamics. Paradoxically, in the case of one-channel time reversal, chaotic dynamics is not only harmless but even useful, as it guarantees ergodicity and mixing. Secondly, using a source of vanishing aperture, there is an almost perfect focusing quality. The procedure approaches the performance of a closed TRM, which has an aperture of 360°. Hence, a one-point time reversal in a chaotic cavity produces better results than a limited aperture TRM in an open system. Using reflections at the edge, focusing quality is not aperture limited; the time-reversed collapsing wavefront approaches the focal spot from all directions.

Although one obtains excellent focusing, a one-channel time reversal is not perfect, as a weak noise level throughout the system can be observed. There is a saturation regime beyond the Heisenberg time. Residual temporal and spatial sidelobes persist even for time-reversal windows of duration larger than the Heisenberg time. They are due to multiple reflections passing over the locations of the TR transducer and they have been expressed in closed form by Draeger and Fink. Using an eigenmode analysis of the wavefield, they explain that, for long time-reversal windows, there is a saturation regime that limits the signal-to-noise ratio (SNR). To evaluate the time-reversed field for the elastic wave in the one-channel experiment we can use Eq. (15) with a TRM located at unique point $\mathbf{r}_{trm}$ and the vertical component of the displacement field $\varphi_{tr}(\mathbf{r}, t)$ is given by (note that the time derivative of Eq. (15) has disappeared because of the dimensionality of the displacement field)

$$\varphi_{tr}(\mathbf{r}, t) \prec G(\mathbf{r}_{trm}, \mathbf{r}_0; -t) \otimes G(\mathbf{r}, \mathbf{r}_{trm}; t) \tag{16}$$

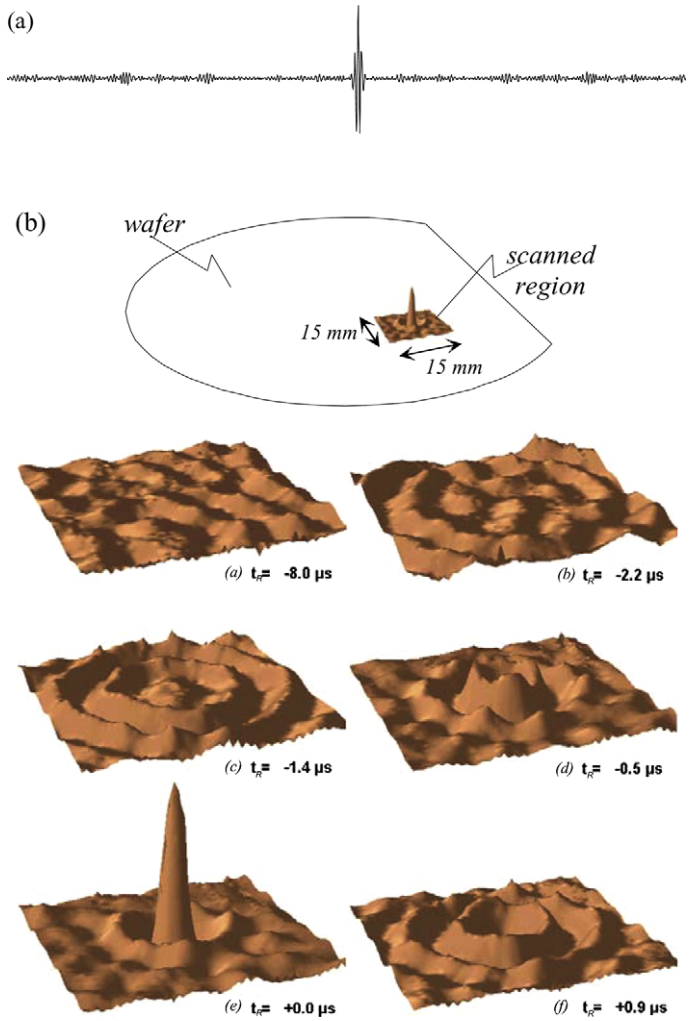

Fig. 4. (a) Time-reversed signal observed at point $\mathbf{r}_0$. The observed signal is 210 µs long. (b) Time-reversed wavefield observed at different times around point $\mathbf{r}_0$ on a square of 15 mm × 15 mm.

Taking into account the modal decomposition of the Green's functions $G(\mathbf{r}, \mathbf{r}_{trm}; t)$ and $G(\mathbf{r}_{trm}, \mathbf{r}_0; -t)$ on each of the eigenmodes $u_j(\mathbf{r})$ of the cavity with eigenfrequency ω_j, we get:

$$G(\mathbf{r}, \mathbf{r}_{trm}; t) = \sum_j u_j(\mathbf{r}) u_j(\mathbf{r}_{trm}) \frac{\sin(\omega_j t)}{\omega_j} \quad (t > 0) \tag{17}$$

Under the assumption that the eigenmodes are not degenerated (valid for a chaotic cavity), we calculate $\varphi_{tr}(\mathbf{r}, t)$ for a time window of duration longer than the Heizenberg time of the cavity and we get

$$\varphi_{tr}(\mathbf{r}, t) \propto \sum_i \frac{1}{\omega_i^2} u_i(\mathbf{r}) u_i(\mathbf{r}_0) u_i^2(\mathbf{r}_{trm}) \cos(\omega_i t) \tag{18}$$

Note that at the focal time $t = 0$ (collapse) the directivity pattern of the time-reversed wavefield is

$$\varphi_{tr}(\mathbf{r}, t) \prec \sum_i \frac{1}{\omega_i^2} u_i(\mathbf{r}) u_i(\mathbf{r}_0) u_i^2(\mathbf{r}_{trm}) \tag{19}$$

Note that in a real experiment one has to take into account the limited bandwidth of the source, so a spectral function $S(\omega)$ centered on center frequency ω_c, with bandwidth $\Delta\omega$, must be introduced and we can write Eq. (19) in the form

$$\varphi_{tr}(\mathbf{r},0)=\sum_i \frac{1}{\omega_i^2}u_i(\mathbf{r})u_i(\mathbf{r}_0)u_i^2(\mathbf{r}_{trm})S(\omega_i) \tag{20}$$

Thus the summation is limited to a finite number of modes, which is typical in our experiment of the order of some hundreds. As we do not know the exact eigenmode distribution for each chaotic cavity, we cannot evaluate this expression directly. However, due to the ergodic properties of the cavity one may use a statistical approach and consider the average over different realizations, which consist in summing over different cavity realizations. So we replace in Eq. (20) the eigenmodes product by their expectation values $\langle\ldots\rangle$. We use also a qualitative argument proposed by Berry [14,15] to characterize irregular modes in chaotic system. If chaotic rays support an irregular mode, it can be considered as a superposition of a large number of plane waves with random direction and phase. This implies that the amplitude of an eigenmode has a Gaussian distribution with $\langle u_i^2\rangle=\sigma^2$ and a short-range isotropic correlation function given by a Bessel function that reads:

$$\big\langle u_i(\mathbf{r})u_i(\mathbf{r}_0)\big\rangle = J_0\big(2\pi|\mathbf{r}-\mathbf{r}_0|/\lambda_i\big) \tag{21}$$

where λ_i is the wavelength corresponding to ω_i. If $\mathbf{r}$ and $\mathbf{r}_0$ are sufficiently far apart from $\mathbf{r}_{trm}$ not to be correlated, then

$$\big\langle u_i(\mathbf{r})u_i(\mathbf{r}_0)u_i^2(\mathbf{r}_{trm})\big\rangle = \big\langle u_i(\mathbf{r})u_i(\mathbf{r}_0)\big\rangle\big\langle u_i^2(\mathbf{r}_{trm})\big\rangle \tag{22}$$

One obtains finally:

$$\big\langle\varphi_{tr}(\mathbf{r},0)\big\rangle=\sum_i \frac{1}{\omega_i^2}J_0\big(2\pi|\mathbf{r}-\mathbf{r}_0|/\lambda_i\big)\sigma^2F(\omega_i) \tag{23}$$

The experimental results obtained in Fig. 4a agree with this prediction and show that in a chaotic cavity the spatial resolution is independent of the time-reversal mirror aperture. Indeed, with a one-channel time-reversal mirror, the directivity patterns at $t=0$ are closed to the Bessel function $J_0(2\pi|\mathbf{r}-\mathbf{r}_0|/\lambda_c)$ corresponding to the central frequency of the transducers. This means that the one-channel time-reversed field is a good estimate of the imaginary part of the Green's function (see Eq. (14)) that was predicted for a closed time-reversal cavity made of large number of antenna.

One can also observe, in Fig. 4b, a very good estimate of the eigenmode correlation function experimentally obtained with only one realization. A one-channel omnidirectional transducer is able to refocus a wave in a chaotic cavity, and if the bandwidth is very large, we do not have to use a TRM made of many transducers.

The focusing process described here is very different from the focusing techniques used in the monochromatic regime. Here, the frequency diversity is use to concentrate the wavefield at *one time* at *one location*. It is interesting to compare this focusing approach for broadband signals with phase conjugation of monochromatic signal. Time reversal of $p(\mathbf{r},t)$ is equivalent, for each spectral component $\hat{P}(\mathbf{r},\omega)$, to complex conjugation. For a single-frequency signal, time reversal is equivalent to complex conjugation of complex amplitude. In a closed cavity, as above, if one works only at a single frequency (say that of one of the eigenmodes ω_i), one constructs only the eigenmode pattern corresponding to the selected frequency. The refocusing process discussed above works only with broadband pulses, over a bandwidth that includes a large number of eigenmodes. Here, the averaging process that gives a good focusing is obtained by a sum over the different modes in the cavity by assuming that in a chaotic cavity, we have a statistical decorrelation of the different eigenmodes, the time-reversed field can be computed by adding the various frequency components (each individual mode) and it can be represented as a sum of Fresnel vectors (Fig. 5). At the source position, all these phase conjugated fields have a zero phase (this comes from the phase conjugation operation that exactly compensates for the forward phase) and even if there is no amplitude focusing for each spectral contributions, there is a constructive interference between all these fields at the focusing time as $\sum_i|\hat{G}(\mathbf{r}_0,\mathbf{r}_{trm};\omega_i)|^2$ where $\hat{G}(\mathbf{r}_0,\mathbf{r}_{trm};\omega)$ is the Fourier transform of $G(\mathbf{r}_0,\mathbf{r}_{trm};t)$. Thus, the total field at the focusing time increases proportionally to the number I of modes (or arrows). Outside the source position, at point $\mathbf{r}$, we observe $\sum_i\hat{G}(\mathbf{r}_0,\mathbf{r}_{trm};\omega_i)\hat{G}^*(\mathbf{r},\mathbf{r}_{trm};\omega_i)$, the contributions of each individual mode are decorrelated because there is no longer coherent phase compensation and therefore the total length only increases as $\sqrt{I}$. On the whole, the focusing peak emerges at the focusing time from the noise when the bandwidth is large enough to contain many different modes. Ideally, if we could indefinitely

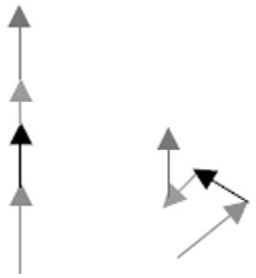

Fig. 5. Schematic representation of a broad-band time-reversal operation at the source (right part) and off the source (left part). Each arrow represents a different Fresnel vector corresponding to a frequency component. At the source position, all the phases are set back to 0, the amplitude of the resulting signal rises proportionally to the number of independent frequencies N. Outside the source, the different contributions are presumably decorrelated, and the standard deviation of their sum rises as $\sqrt{N}$.

expand the bandwidth, the background level on the directivity patterns should decrease as $1/\sqrt{I}$. As the number of eigenfrequencies available in the transducer bandwidth increases, the refocusing quality becomes better and the focal spot pattern becomes closed to the ideal Bessel function.

As a conclusion, it must be emphasized that in a closed cavity a one-channel time-reversal mirror can focus with $\lambda/2$ resolution if the duration of the time-reversal window is greater or equal to the cavity's Heisenberg time. Longer time windows do not improve the focusing quality. However, a larger bandwidth $\Delta\omega$ reduces the side lobe levels as $1/\sqrt{\Delta\omega}$.

Time reversal in reverberant cavities at audible frequencies has been shown to be an efficient localizing technique in solid objects. The idea consists in detecting acoustic waves in solid objects (for example, a table or a glass plate) generated by a slight finger knock. As in a reverberating object, a one-channel TRM has the memory of many distinct source locations, and the information location of an unknown source can then be extracted from a simulated time-reversal experiment in a computer. Any action, turn on the light or a compact disk player, for example can be associated with each source location. Thus, the system transforms solid objects into interactive interfaces. Compared to the existing acoustic techniques, it presents the great advantage of being simple and easily applicable to inhomogeneous objects whatever their shapes. The number of possible touch locations at the surface of objects is directly related to the number of independent time-reversed focal spots that can be obtained. For example, a virtual keyboard can be drawn on the surface of an object; the sound made by fingers when a text is captured, is used to localize impacts. Then, the corresponding letters are displayed on a computer screen [16].

3.2. Time reversal in open systems: random media

The ability to focus with a one-channel time-reversal mirror is not only limited to experiments conducted inside closed cavity. Similar results have also been observed in time-reversal experiments conducted in open random medium with multiple scattering [17–19]. A. Derode et al. carried out the first experimental demonstration of the reversibility of an acoustic wave propagating through a random collection of scatterers with strong multiple scattering contributions. A multiple scattering sample is immersed between the source and a TRM array made of 128 elements. The scattering medium consists of 2000 randomly distributed parallel steel rods (diameter 0.8 mm) arrayed over a region of thickness $L = 40$ mm with average distance between rods 2.3 mm. The elastic mean free path in this sample was found to be 4 mm (see Fig. 6). A source 30 cm from the 128 elements TRM transmitted a short (1 μs) ultrasonic pulse (3 cycles of 3.5 MHz, $\Delta\omega = 1$ MHz).

Fig. 7a shows one part of the waveform received by one element of the TRM. It spread over more than 200 μs, i.e. 200 times the initial pulse duration. After the arrival of a first wavefront corresponding to the ballistic wave, a long diffuse wave is observed due to the multiple scattering. In the second step of the experiment, any number of signals (between 1 and 128) is time-reversed and transmitted and a hydrophone measures the time-reversed wave in the vicinity of the source. For a TRM of 128 elements, with a time-reversal window of 300 μs, the time-reversed signal received on the source is represented in Fig. 7b: an impressive compression is observed, since the received signal lasts about 1 μs, against over 300 μs for the scattered signals. The directivity pattern of the TR field is also plotted in Fig. 8. It shows that the resolution (i.e. the beam width around the source) is significantly finer than it is in

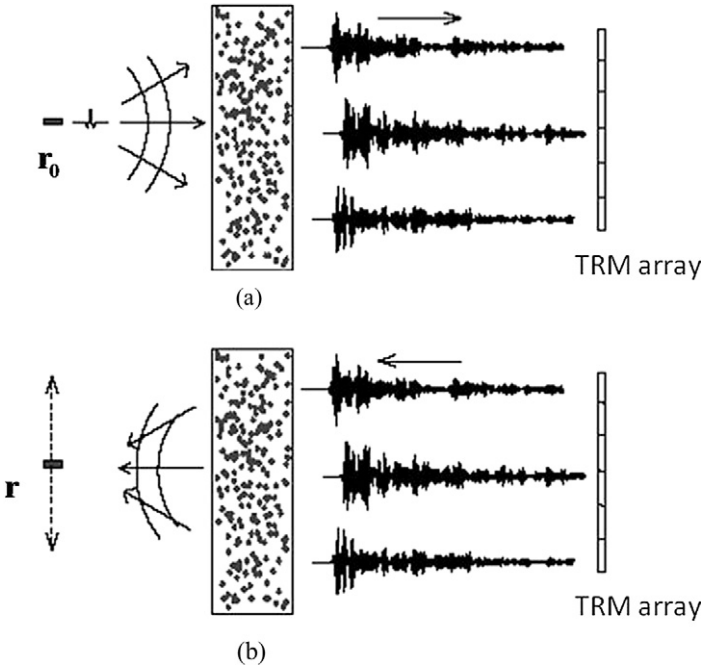

Fig. 6. Time-reversal focusing through a random medium. In the first step the source $\mathbf{r}_0$ transmits a short pulse that propagates through the rods. The scattered waves are recorded on a 128-element array. In the second step, N elements of the array ($0 < N < 128$) retransmit the time-reversed signals through the rods.The piezoelectric element located at $\mathbf{r}_0$ is now used as a detector, and measures the signal reconstructed at the source position. It can also be translated along the x-axis while the same time-reversed signals are transmitted by the array, in order to measure the directivity pattern.

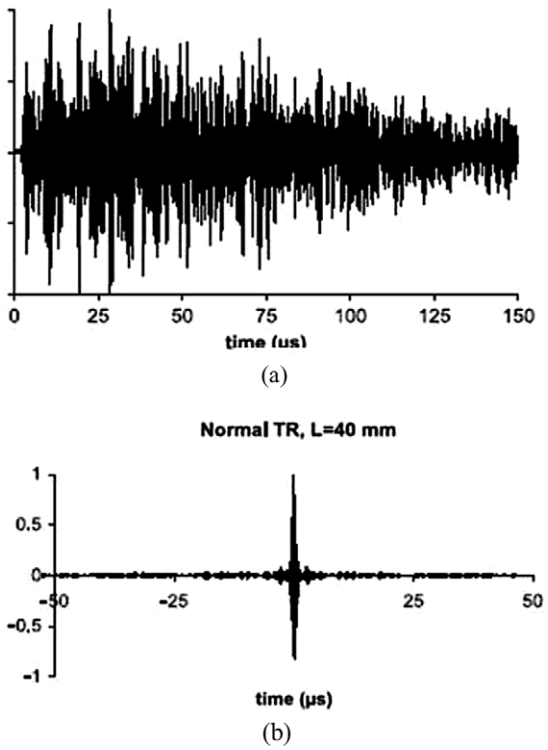

Fig. 7. Experimental results. (a) Signal transmitted through the sample ($L = 40$ mm) and recorded by the array element no. 64, and (b) signal recreated at the source after time reversal.

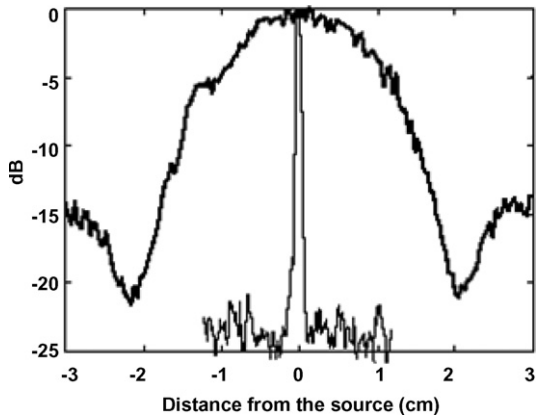

Fig. 8. Directivity pattern of the time-reversed waves around the source position, in water (thick line) and through the rods (thin line), with a 16-element aperture. The sample thickness is $L = 40$ mm. The -6 dB widths are 0.8 and 22 mm, respectively.

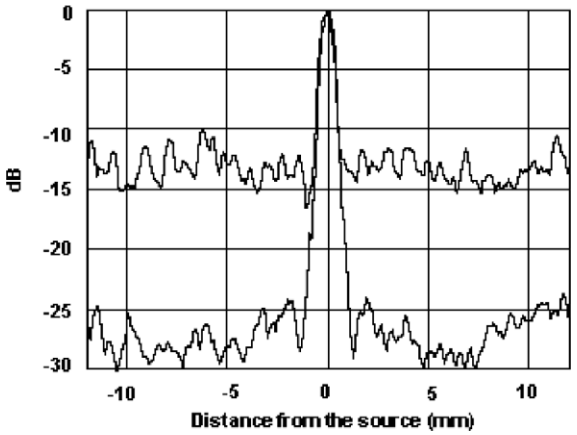

Fig. 9. Directivity pattern of the time-reversed waves around the source position through $L = 40$ mm, with $N = 128$ transducers (thin line) and $N = 1$ transducer (thick line). The -6 dB resolutions are 0.84 and 0.9 mm, respectively.

the absence of scattering: the resolution is 30 times finer, and the background level is below -20 dB. Moreover, Fig. 9 shows that the resolution is independent of the array aperture: even with only one transducer doing the time-reversal operation, the quality of focusing is quite good and the resolution remains approximately the same as with an aperture 128 times larger. This is clearly the same effect as observed with the closed cavity. High transverse spatial frequencies of arbitrary k that would have been lost in a homogeneous medium are redirected by the scatterers towards the array. Once again this result illustrates the difference between phase conjugation and time reversal. If the experiment had been quasi-monochromatic and the single array element had simply phase conjugated one frequency component, the conjugated wavefield would never have focused on the source position. Indeed, whatever its phase, there is no reason for a monochromatic wave emanating from a point source to be focused in a particular place on the other side of a random sample. The phase conjugated field at one frequency in the source plane is perfectly random and verifies the classical speckle distribution.

As for a broadband signal in a closed cavity, an analysis similar to that of the last paragraph can be conducted in order to predict the level of the side lobes around the focal peak. A modal decomposition of the field is not directly applicable. However, if we keep in mind that the focusing with one channel occurs only for a broadband transducer, we identify the number of uncorrelated spectral correlation length $\delta\omega$ of the scattered waves. Then there are $\Delta\omega/\delta\omega$ uncorrelated bits of spectral information in the frequency bandwidth, and the signal-to-noise is expected to vary like $\sqrt{\Delta\omega/\delta\omega}$. To evaluate the spectral correlation length, one can use the Wiener–Kinchin theorem [18] that gives

the spectral correlation function (averaged over the frequency bandwidth) as the Fourier transform of the 'time of flight' distribution. In a multiply scattering medium, in the diffusive approximation, it is well known that the typical spreading time (the so-called Thouless time) is equal to $\tau_{Thouless} = L^2/D$ where D is a diffusion coefficient related to the mean free path and L is the thickness sample. Therefore $\delta\omega = D/L^2$, so the number of uncorrelated frequencies grows with L^2, provided we can neglect dissipation effects ($\tau_{dissipat} \geqslant \tau_{Thouless}$) where $\tau_{dissipat}$ is the dissipative time.

4. Focusing microwaves below the diffraction limit

Super-resolution can be achieved with an acoustic sink but it has a severe drawback. It needs to use an active source at the focusing point to exactly cancel the usual diverging wave created during the focusing process. Since we know that the time-reversal focusing spot at each frequency depends on the imaginary part of the Green function for any heterogeneous medium, another approach consists in surrounding the focusing point by a microstructured medium with length scales well below the wavelength; strong resonating scatterers were placed in the near-field of the source. In this case, the microstructured medium strongly modifies the spatial dependence of the imaginary part of the Green function that now oscillates on scales much smaller than the wavelength. For a broadband pulse with enough frequency diversity, a time reversal will generate at the focal time an interference between the imaginary part of the Green's function at each frequency (see Eq. (13)). At the source point, the time-reversed field is directly proportional to the number of modes excited inside the microstructure from the source. While at the other points, the oscillations of the imaginary parts at different frequencies cancel their effects. To predict the behaviour of time reversal in such medium, we have to know the field correlations. A wave propagating in any medium can be characterized by a spatial correlation length and a spectral correlation length which have a pretty simple meaning. The spatial correlation length of a medium represents, at a given frequency, the smallest distance between two points which exhibits statistically different wavefields, while the spectral correlation frequency $\delta\omega$ measures the minimal frequency change that leads to independent wavefields. If the correlation length of the medium is much smaller than the wavelength, and if we use a bandwidth that contains several spectral correlation lengths, one can achieve a focusing on a scale of the order of the correlation length of the medium.

This is exactly the idea we exploit in the field of time reversal with microwaves [20] to create focal spots much thinner than the wavelength. In a recent experiment [21] we consider 8 possible focusing points placed in a strong reverberating chamber (Fig. 10a). Eight electromagnetic sources are placed at these 8 locations to be used in the learning step of the TR process. These sources consist of wire antennas used at a central frequency of 2.45 GHz (i.e., $\lambda = 12$ cm), with a bandwidth of 100 MHz. The pitch between them is $\lambda/30$! These eight antennas form an array which will be referred to as the receiving array. Each antenna in this array is surrounded by a microstructure consisting here of a *random distribution of thin copper wires* (Fig. 10b). The mean distance between the thin copper wires was of the order of 1 mm (correlation length $\lambda/100$), while the frequency correlation $\delta\omega$ was of the order of 30 MHz, resulting in three independent speckle patterns in the whole bandwidth. A TRM made of eight commercial dipolar antennas is placed in the far-field, ten wavelengths apart from the receiving array. The set "reverberant chamber/TRM" acts as a *virtual far-field time-reversal cavity*. When antenna marked #3 in Fig. 10 sends a short electromagnetic pulse (10 ns), the 8 signals received at the TRM are much longer than the initial pulse due to strong reverberation in the chamber (typically 500 ns). As an example the signal received at one of the antennas of the TRM is shown in Fig. 11a. When the antenna marked #4 is in its turn used as a source, it is remarkable to point out that now the signal received at the same antenna in the TRM (shown in Fig. 11b) looks significantly different although sources #3 and #4 were $\lambda/30$ apart from each other. When these signals are time-reversed and transmitted back, the resulting waves converge respectively to antenna #3 and #4 where they recreate pulses as short as the initial ones (Figs. 11c and 11d). Measuring the signal received at the other antennas of the receiving array gives access to the spatial focusing around antennas #3 and #4 (Fig. 11e). The remarkable result is that the two antennas can be addressed independently since the focusing spots created around them have a size much less than the wavelength (here typically $\lambda/30$): the diffraction limit is overcome although the focusing points are in the far-field of the TRM!

Contrary to the acoustic sink experiment, in the microwave time-reversal experiment, the source remains passive and high spatial frequency components of the field are created upon scattering at the disordered structure. Reciprocity ensures that the time-reversed scattering process creates a subwavelength focus around the source location [22]. The initial evanescent waves created around the initial wire are converted into propagating waves by the random distri-

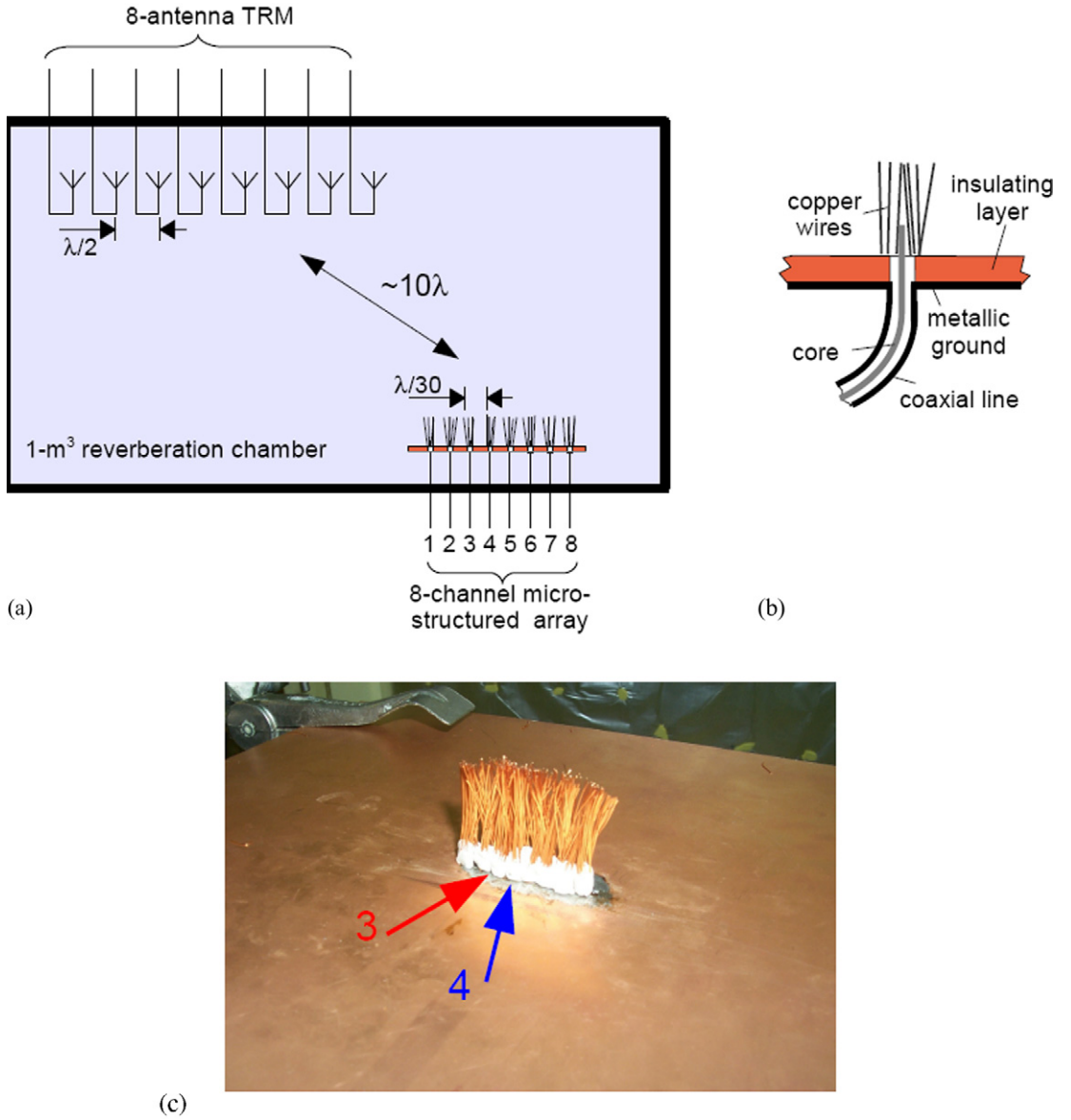

Fig. 10. (a) A time-reversal mirror (TRM) made of eight commercial dipolar antennas operating at 2.45 GHz with 100 MHz bandwidth (i.e., $\lambda = 12$ cm) is placed in a 1-m^3 reverberating chamber. Ten wavelengths away from the TRM is placed a subwavelength receiving array, consisting of eight microstructured antennas $\lambda/30$ apart from one another. (b) Details of one microstructured antenna. It consists of the core of a coaxial line which comes out 2 mm from an insulating layer and is surrounded by a microstructure consisting of a random distribution of thin copper wires. (c) Photo of the 8-element subwavelength array surrounded by the random distribution of copper wires. Antennas #3 and #4 are indicated by the red and blue arrows. (For interpretation of the references to color in this figure legend, the reader is referred to the web version of this article.)

bution of wires. In the time-reversed step, these propagating waves are playback, from the far field, with reverse $\vec{k}$. Spatial reciprocity ensures that each propagating waves with a reverse $\vec{k}$ interact with the random distribution of wires to recreate the initial evanescent waves around the focus.

Note that this approach can work not only when the experiment is conducted inside a reverberant cavity [23]. Provided, the microstructured medium generates enough multiple scattering in the near field of the source resulting in a transmitted signal sufficiently long, the time-reversal signal from a small TRM located in free space leads to beat the diffractions limit.

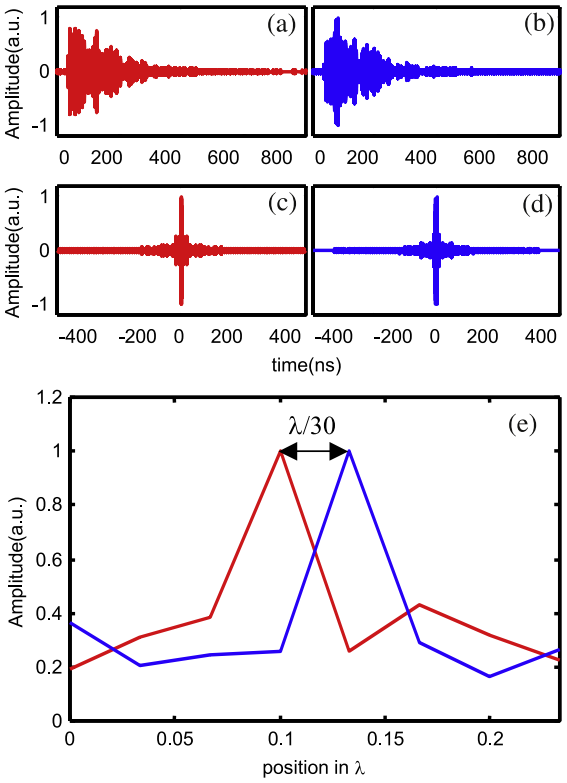

Fig. 11. In (a) (resp. (b)) is shown the signal received at one antenna of the TRM when a 10-ns pulse is sent from antenna #3 (resp. #4) of the subwavelength array. The signals in (a) and (b) look significantly different although antenna #3 and antenna #4 are distant from $\lambda/30$. In (c) (resp. (d)) is shown the time compression obtained at antenna #3 (resp. #4) obtained when the eight signals coming from antenna #3 (resp. antenna #4) are time-reversed and sent back from the TRM. In (e) are shown the focusing spots obtained around antennas #3 and #4. Their width is $\lambda/30$. Thus antennas #3 and #4 can be addressed independently.

5. Conclusion

We have shown that in presence of multiple reflections or multiple scattering, a small size time-reversal mirror manages to focus a pulse back to the source with a spatial resolution that beats the diffraction limit. The resolution is no longer dependent on the mirror aperture size but it is only limited by the spatial correlation of the wavefield. In these media, due to a sort of kaleidoscopic effect that creates virtual transducers, the TRM appears to have an effective aperture that is much larger than its physical size. Resolution can be improved in reverberating media using this concept. Time-reversal focusing opens also completely new approaches to super-resolution. We have shown that in a medium made of random distribution of subwavelength scatterers, a broadband time-reversed wavefield interacts with the random medium to regenerate not only the propagating but also the evanescent waves required to refocus below the diffraction limit. Focal spots as small as $\lambda/30$ have been demonstrated with microwaves. This results in a large increase of the information transfer rate by time reversal in such disordered media.

References

[1] M. Fink, IEEE Trans. Ultrason. Ferroelec. Freq. Contr. 39 (5) (1992) 555–566.
[2] M. Fink, Phys. Today 50 (3) (1997) 34–40.
[3] M. Fink, D. Cassereau, A. Derode, C. Prada, P. Roux, M. Tanter, J.L. Thomas, F. Wu, Rep. Prog. Phys. 63 (12) (2000) 1933–1995.
[4] D. Cassereau, M. Fink, IEEE Trans. Ultrason. Ferroelec. Freq. Contr. 39 (5) (1992) 579–592.
[5] D.R. Jackson, D.R. Dowling, J. Acoust. Soc. Am. 89 (1) (1991) 171–181.
[6] J. de Rosny, M. Fink, Phys. Rev. Lett. 89 (12) (2002) 124301.
[7] D.-J. van Manen, J. Robertsson, A. Curtis, Phys. Rev. Lett. 94 (2005) 164301.
[8] M. Nieto-Vesperinas, E. Wolf, J. Opt. Soc. Am. A 2 (9) (1985) 1429–1434.

[9] R. Weaver, J. Acoust. Soc. Am. 71 (1982) 1608–1609.
[10] K.J. Ebeling, in: W.P. Mason (Ed.), Physical Acoustics, vol. 17, Academic, New York, 1984, pp. 233–309.
[11] C. Draeger, M. Fink, Phys. Rev. Lett. 79 (3) (1997) 407–410.
[12] C. Draeger, M. Fink, J. Acoust. Soc. Am. 105 (2) (1999) 618–625.
[13] C. Draeger, J.-C. Aime, M. Fink, J. Acoust. Soc. Am. 105 (2) (1999) 611–617.
[14] M.V. Berry, Chaotic Behaviour of Deterministic Systems, Les Houches, North Holland, Amsterdam, 1981, pp. 171–271.
[15] S.W. McDonald, A.N. Kaufman, Phys. Rev. A 37 (8) (1988) 3067–3086.
[16] R.K. Ing, N. Quieffin, S. Catheline, M. Fink, Appl. Phys. Lett. 87 (20) (2005), Art. No. 204104.
[17] A. Derode, P. Roux, M. Fink, Phys. Rev. Lett. 75 (23) (1995) 4206–4209.
[18] A. Derode, A. Tourin, M. Fink, Phys. Rev. E 64 (3) (2001) 36606.
[19] P. Blomgren, G. Papanicolaou, H. Zhao, J. Acoust. Soc. Am. 111 (1) (2002) 230–248.
[20] R. Carminati, R. Pierrat, J. de Rosny, M. Fink, Opt. Lett. 32 (2007) 3107–3109.
[21] G. Lerosey, J. de Rosny, A. Tourin, M. Fink, Science 315 (2007) 1120.
[22] R. Carminati, J. Sáenz, J. Greffet, M. Nieto-Vesperinas, Phys. Rev. A 62 (2000) 012712.
[23] X. Li, M.I. Stockman, Phys. Rev. B 77 (2008) 195109.